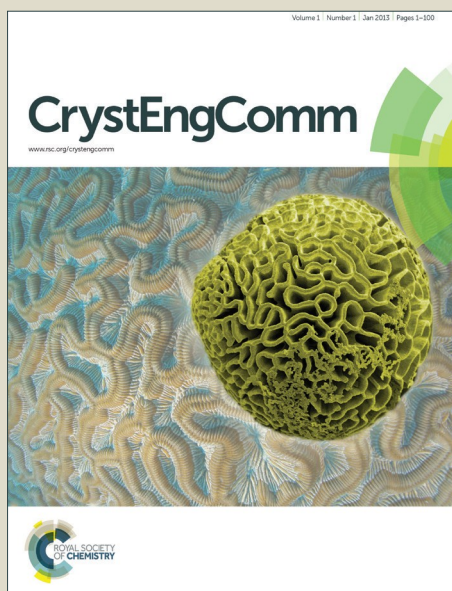


# CrystEngComm

Accepted Manuscript



This is an *Accepted Manuscript*, which has been through the Royal Society of Chemistry peer review process and has been accepted for publication.

*Accepted Manuscripts* are published online shortly after acceptance, before technical editing, formatting and proof reading. Using this free service, authors can make their results available to the community, in citable form, before we publish the edited article. We will replace this *Accepted Manuscript* with the edited and formatted *Advance Article* as soon as it is available.

You can find more information about *Accepted Manuscripts* in the [Information for Authors](#).

Please note that technical editing may introduce minor changes to the text and/or graphics, which may alter content. The journal's standard [Terms & Conditions](#) and the [Ethical guidelines](#) still apply. In no event shall the Royal Society of Chemistry be held responsible for any errors or omissions in this *Accepted Manuscript* or any consequences arising from the use of any information it contains.

Ameliorated synthetic methodology of crystalline lanthanoid-metalloporphyrin open frameworks based on the multi-topic octacarboxy-porphyrin scaffold; structural, gas sorption and photophysical properties<sup>¶</sup>

B. K. Tripuramallu, H. M. Titi, S. Roy, R. Verma and I. Goldberg\*

*School of Chemistry, Sackler Faculty of Exact Sciences, Tel-Aviv University, Ramat-Aviv, 6997801 Tel-Aviv, Israel.*

*E-mail: aryanbharat@gmail.com, goldberg@post.tau.ac.il*

**New crystalline lanthanoid-metalloporphyrin porous frameworks [(Zn(H<sub>2</sub>O)-OCPP)Ln<sub>2</sub>(H<sub>2</sub>O)<sub>4</sub>Na<sub>2</sub>]<sub>n</sub>-solvent (Ln = Sm, Eu, Gd, Tb, Dy) (LnMPF-1) were synthesized from the octa-topic tetrakis-(3,5-dicarboxyphenyl)porphyrin building block through a synthetic approach using NaOH as a modulator to enhance the robustness of the metal-organic-framework (MOF) product and the formation of sizeable crystals. The formulated MOFs adopt a (4,8) connected topology and are perforated by 1D tubular zigzag channels about 1.5 nm in diameter. The frameworks possess permanent porosity and display appealing photophysical properties.**

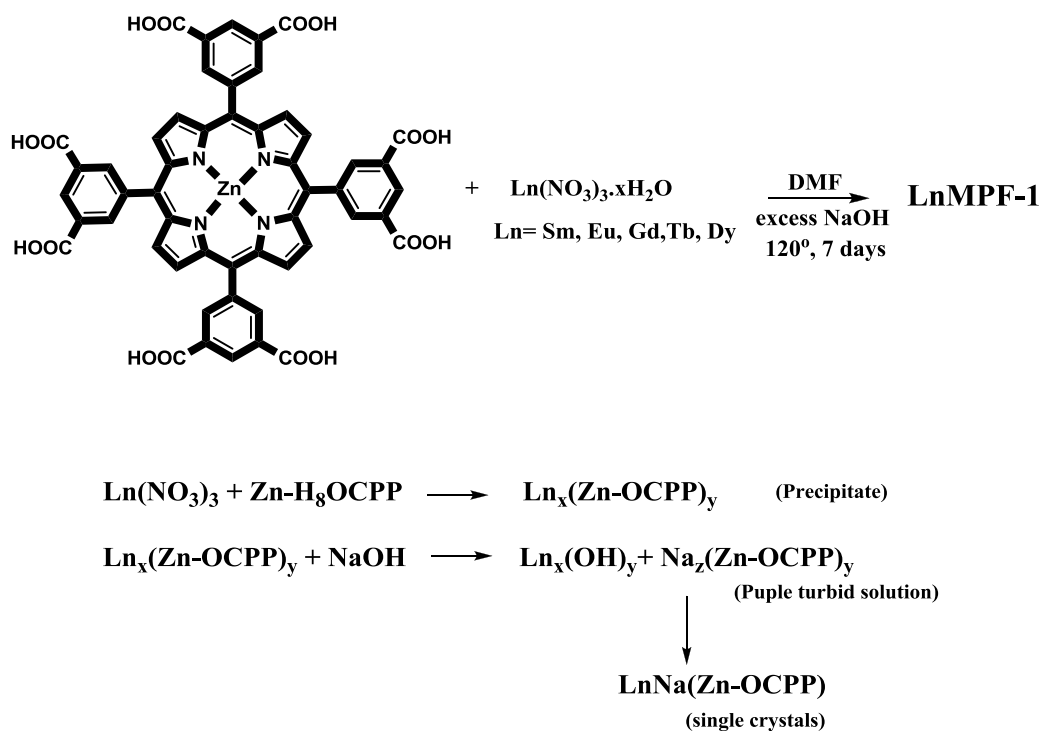
The porphyrins and their structurally related molecules are abundant compounds in a variety of natural and artificial processes.<sup>1</sup> They provide also very attractive building blocks for the construction of diverse hybrid materials in different branches of science.<sup>2</sup> The porphyrin-based metal organic frameworks or metalloporphyrin frameworks are unique in terms of transforming the distinctive geometrical and photo-physical features associated with porphyrin molecules to the potential applications in the fields of light harvesting, oxygen transport, catalysis and other areas.<sup>3</sup> Facile synthetic modification of the porphyrin macrocycles with functional groups (in particular at the *meso* positions) allows targeting frameworks of desired architectures, porosity, thermal stability and reactivity.<sup>4,5</sup> The metalloporphyrin frameworks have been also widely used as model compounds to mimic the natural photosynthetic process,<sup>3</sup> and their light harvesting potential could be further enhanced through sensitization of the framework surface by quantum dots.<sup>6</sup> The lanthanoid ions and clusters of ions can serve as excellent connecting nodes (secondary building units

- SBUs) in the assembly process of multiporphyrin architectures. They are hard acids and exhibit strong tendency to bind oxygen atoms of coordinating groups, as e.g., carboxylates, phenolates or sulphonates. Lanthanoid-supported metal organic frameworks (LnMOFs) have been widely explored as promising candidates for materials with intriguing architectures and displaying unusual magnetic behaviors and color-tunable luminescence.<sup>7</sup> Formulations and characterizations of LnMOFs involving tetraarylporphyrin linkers have enjoyed a rather slow progress in view of the synthetic difficulty in obtaining sizeable crystalline specimens, as polycrystalline or amorphous solids are most frequently the outcome of common preparative procedures. In the latter context, we reported earlier on the synthesis of framework solids of tetra(3/4-carboxyphenyl)porphyrin (TCPP) scaffolds with lanthanoid ions.<sup>8</sup> More recently, fixation of CO<sub>2</sub> in 2D lanthanide-TCPP networks has been discussed as well.<sup>9</sup> Other reports elaborated on MOFs based on the tetra(4-sulfonatophenyl)porphyrin and lanthanoid ions and on the photophysical properties of the resulting frameworks.<sup>10</sup> The synthetic difficulties of porphyrin-based MOFs supported by lanthanoid connectors limit their potential utility in areas related to gas sorption applications and as photoluminescent materials.<sup>11</sup> Hence, the design of porphyrin-based crystalline LnMOFs displaying permanent porosity and retaining characteristic emissions of porphyrins remains a challenging task. The multitopic porphyrin building block zinc-tetrakis-(3,5-dicarboxyphenyl)porphyrin (Zn-H<sub>8</sub>OCPP) is reported to form highly porous metal-metalloporphyrin frameworks with first row transition metals, and these frameworks act as good catalysts for selective oxidations and coupling reactions.<sup>12</sup> However, reactions of this octa-topic scaffold with exocyclic metal centers (and in particular with the oxophilic lanthanoid ions) readily yields amorphous precipitates or at best micro crystalline phases. In the latter case, structural characterizations of the H<sub>8</sub>OCPP-based MOFs by X-ray diffraction techniques require access to synchrotron radiation sources (due to the weak diffraction power of the small crystallites and high content of disordered solvent trapped in the lattice), and are considerably more elaborate and scarce.<sup>12a,12e-f</sup> As part of our continuous efforts to design porous porphyrin-based MOFs we report in this paper on a reliable and optimized synthetic methodology to this end, and describe the first example of a porous 3D framework constructed successfully by reacting various Ln-ions with the Zn-H<sub>8</sub>OCPP metallo-porphyrin (LnMPF-1). A series of isostructural crystalline materials [(Zn(H<sub>2</sub>O)-OCPP)Ln<sub>2</sub>(H<sub>2</sub>O)<sub>4</sub>Na<sub>2</sub>]<sub>n</sub>·solvent [Ln= Gd (**1**), Sm (**2**), Dy (**3**), Eu (**4**), Tb (**5**)] were obtained, characterized by a (4,8)-connected network topology. Sodium hydroxide has been used as a modulator in the formation of sizeable LnMPF

crystals of permanent porosity by decreasing the rate of the supramolecular reaction between porphyrin scaffold and the lanthanoids, through formation of lanthanoid-hydroxide intermediates.

Solvothermal reactions of  $\text{Ln}(\text{NO}_3)_3 \cdot x\text{H}_2\text{O}$  with  $\text{Zn-H}_8\text{OCPP}$  in DMF at  $120^\circ\text{C}$  in the presence of excess NaOH gave single crystals of LnMPF-1. Initially lanthanide nitrates and  $\text{Zn-H}_8\text{OCPP}$  were dissolved in DMF and heated at  $120^\circ\text{C}$  for two hours, which resulted in the formation of a bulky purple precipitate with clear colorless solution. The latter indicated that all the  $\text{Zn-H}_8\text{OCPP}$  starting material reacted with the inorganic salt. To this precipitate 1M NaOH was added and sonicated for few minutes to yield a purple-colored turbid solution. The addition of the base breaks the lanthanide-porphyrin precipitate to form lanthanide hydroxide species, releasing the porphyrin molecules into the solution. This turbid solution was then heated at  $120^\circ\text{C}$  for 7 days, yielding single crystals of LnMPFs, in which sodium ions were also incorporated into the metal-organic-framework. In the latter step the carboxylate groups of porphyrin molecules slowly replace the hydroxide ligands in the lanthanide coordination sphere and form the required crystalline LnMPFs. The NaOH reagent plays a multiple role in the reaction process. The basic environment facilitates deprotonation of the carboxylic functions for ready coordination to the Ln-centers. Then, the hydroxyl ions compete with the carboxylate anions for coordinating to the metal, thus slowing the reaction rate between the lanthanoid and the porphyrin, and thus enhancing crystal growth of the solid product. Finally the sodium cations are incorporated into the MOF to account for charge balance, due to the imparity between the tri-valent lanthanoid node and tetra-anionic (in the strongly basic environment) porphyrin linker. The mediating effect of the NaOH is further evident from the strong correlation between its concentration and the size of the crystallites that form. As the concentration of NaOH increases, the form of the product changes from microcrystalline grains to sizeable single crystals. At the initial stage purple precipitate was formed for a short period in the absence of NaOH. As shown in Fig. 1, when 100  $\mu\text{L}$  of 1N NaOH was added a purple microcrystalline product was formed along with large amount of colorless lanthanum hydroxide crystals. Increasing the amount of the added NaOH to 200  $\mu\text{L}$  led to the formation of larger crystals, but still too small for effective diffraction experiments on home-lab equipment. At the third stage the amount of added NaOH was maintained between 300 to 400  $\mu\text{L}$  (i.e nearly 20 equivalents with respect to that of the  $\text{Zn-H}_8\text{OCPP}$  reactant), which led finally to block-shaped and sizeable (e.g.,  $\sim 0.20 \times 0.20 \times 0.12 \text{ mm}^3$ ) crystals of the desired MOF. Scheme 1 shows the proposed reaction pathway of the LnMPFs synthesis. Behrens *et*

*al.* reported the modulated synthesis approach for preparation of crystalline Zr-MOFs using benzoic acid as a modulator and this method was well exploited by several groups to obtain several Zr-MOFs<sup>13</sup> and other Zr-porphyrin systems.<sup>14</sup> In this context the proposed synthetic approach lay down a pathway to obtain crystalline lanthanide frameworks from multitopic building blocks.



**Scheme 1** Methodology adopted to synthesize LnMPF-1 and the plausible reaction phases in obtaining the crystalline materials.

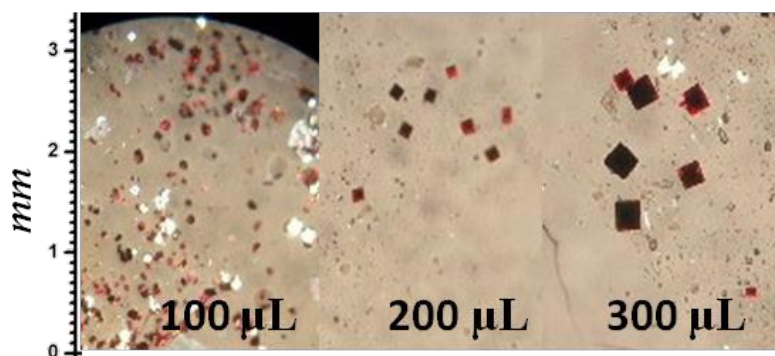


**Fig. 1** Illustration demonstrating the influence of NaOH concentration in the supramolecular reaction on the crystal size of the resulting product

All the crystalline materials with the various lanthanoid ions Gd, Sm, Dy, Eu and Tb are isostructural (see in Supporting Information). Single crystal X-ray analysis revealed that all the LnMPFs crystallize in space group *Imma* and form the same type of the 3D porous metal organic framework, and the following discussion of its architecture will refer therefore to the representative best-diffracting Gd-derivative. The corresponding crystal structure can be best described in a modular way. Coordination of carboxylate groups from OCPP<sup>8-</sup> to the Gd and Na metal centers forms 1D polymeric chain that propagates along the *c*-axis of the crystal (Fig. 2a). The repeating unit along these chains consists of {NaGd(H<sub>2</sub>O)<sub>2</sub>(COO<sup>-</sup>)<sub>4</sub>}synthons. The Gd ion is eight-coordinate to two carboxylate groups of different porphyrin entities in a bidentate manner, two other carboxylate residues in a mono-dentate fashion and to two molecules of water. The Na ions have a tetrahedral coordination environment binding to four different carboxylates in a mono-dentate fashion.. The fully deprotonated Zn-H<sub>8</sub>OCPP tetra-acid moiety inter-connects between four neighboring {NaGd(H<sub>2</sub>O)<sub>2</sub>(COO<sup>-</sup>)<sub>4</sub>}<sub>n</sub> chains. The resulting residue resembles an open molecular box, wherein the porphyrin macrocycles make the bottom and top surfaces, and the {NaGd(H<sub>2</sub>O)<sub>2</sub>(COO<sup>-</sup>)<sub>4</sub>} subunits link between them along the four edges of the box (Fig. 2b). The top-to-bottom distance between the Zn-centers is 13.1 Å and the (atom-to-atom) opening between edges in a perpendicular direction is 12.2 Å. This box-like pattern extends throughout the crystal, forming a 3D polymeric framework perforated by one-dimension channel-type voids that propagate along the *a*-axis of the crystal. Adjacent "molecular boxes" are staggered with respect to each other. This mode of connectivity imparts zig-zag nature to the channel voids and an increased pore window of about 1.5 nm (Fig.s 2c and S1). The solvent accessible voids within the LnMPF-1 MOF account for 59% of the crystal volume (as assessed by the PLATON software),<sup>15</sup> and are accommodated by disordered molecules of the DMF solvent.

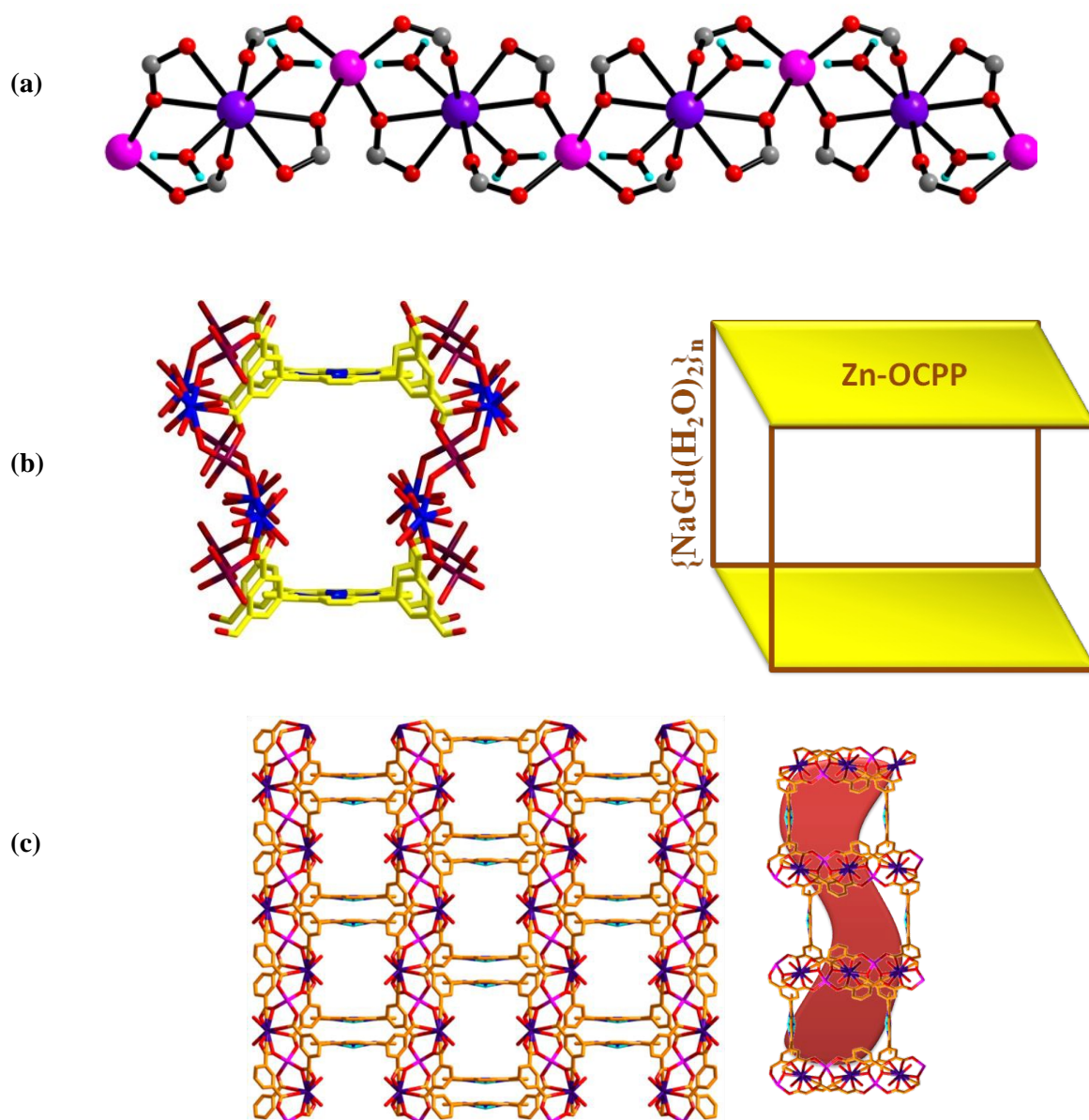


**Fig. 2** Single crystal X-ray structure of LnMPF-1 displaying (a) fragment of  $\{\text{NaGd}(\text{H}_2\text{O})_2(\text{COO}^-)_4\}_n$  1D chains running through the crystal lattice (Gd-violet, Na-pink). (b) The molecular box fragment of the structure involving the porphyrin linkers and the bimetallic nodes. (c) The 3D framework structure of Gd-MPF and 1D zig-zag chains (viewed through *b*-axis) with  $\sim 1.5$  nm pore opening.

In order to reduce the complexity of the topological description to a simpler node-and-linker network, LnMPF-1 was fragmented into the Zn-OCPP<sup>8-</sup> linker, and two Gd- and Na-nodes. Fig. 3 illustrates that every Zn-OCPP<sup>8-</sup> moiety (green) is an

eight connected node, Gd-ion (red) and Na-ion (yellow) as four connected nodes. Each of the metallic nodes (Gd and Na) is coordinated to two porphyrin centers and two adjacent (structurally equivalent) metal ions. The metal clusters generate 1D helical chains arranged in different orientations, clock wise and anti-clock wise (Fig. S2). The topology of LnMPF-1 can be best described as a (4,8)-connected 2-nodal net with Schläfli symbol  $\{4.5^3.6^2\}_4\{4^4.5^4.6^{16}.8^4\}$ . In addition, the framework exhibits the existence of one primitive proper tiling (PPT) with 10 nodes and 24 edges in the repeat unit. The PPT consists of three kinds of tiles corresponding to the  $4[4.6^2]$ ,  $[6^4]$  and  $2[5^4.6^2]$  presentation (Fig. 3).<sup>16</sup>

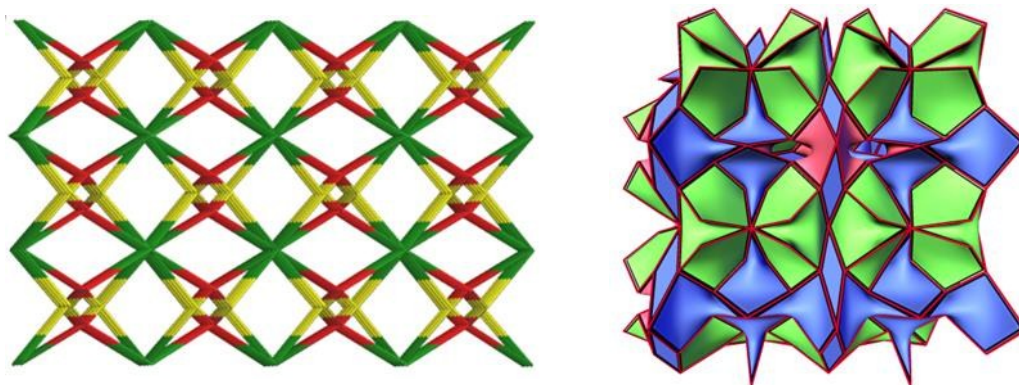


**Fig. 3** Topological representation of (4,8)-connected 2-nodal net of LnMPF-1 (left), and its primitive proper tiling (PPT) of the 3-periodic net (right).<sup>[16]</sup>

TGA studies performed on fresh crystals of GdMPF-1 (Fig. S3) reveal the loss of DMF solvent molecules from the lattice cavities and of the coordinated water molecules from the  $\{\text{NaGd}(\text{H}_2\text{O})_2\}_n$  chains in the range of 30° to 300°C, with weight loss of nearly 40 %. The framework is stable up to 400°C, and collapses above this temperature. The permanent porosity of GdMPF-1 was characterized by gas adsorption measurement at 77k. The as-synthesized GdMPF-1 was washed with DMF and soaked in methanol for two days with occasional swirling to exchange the DMF molecules and then it was preheated at 353K. This was followed by evacuation under dynamic vacuum for 6 hr to generate an activated sample. The phase purity of GdMPF-1 after solvent exchange was confirmed from the PXRD studies and shown in the Fig. S4. The  $\text{N}_2$  adsorption isotherm displays characteristic Type 1 adsorption



isotherm, showing pore condensation with adsorption-desorption hysteresis (Fig. 4a). The hysteresis indicates the microporous nature of the framework with a maximum N<sub>2</sub> uptake of 124 cm<sup>3</sup> g<sup>-1</sup> (STP) at P/P<sub>0</sub>=0.99 relative pressure. The corresponding surface area calculated using the Langmuir equation is 200 m<sup>2</sup>/g. The amount of hydrogen adsorbed, as calculated from the hydrogen adsorption isotherm (Fig. 4b) at normal pressure and at 77 K, is 0.9 wt%. In general, porphyrin frameworks suffer from the collapse of the framework upon removal of solvent molecules.<sup>12a</sup> In the present case, however, the adsorption behavior of GdMPF-1 shows permanent porosity comparable to that reported by Chen et al. for UTSA-57.<sup>17</sup>

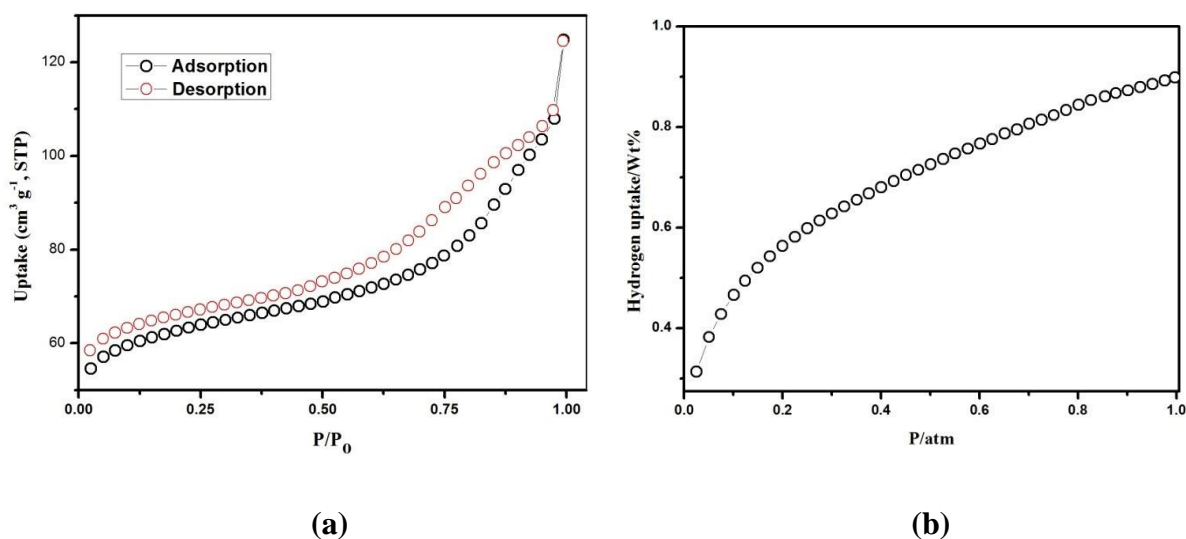


**Fig. 4** (a) N<sub>2</sub> and (b) H<sub>2</sub> adsorption isotherms of GdMPF-1 at 77K.

The ordered arrangement of porphyrin-like pigments is known to be responsible for the energy migration in the natural photosynthetic process. In this respect, the LnMPF-1s reported here possess well-organized arrangement of the organic building block (Zn-OCPP<sup>8-</sup>) and the metal centers in the framework architectures. The optical properties of the LnMPF-1s have been characterized by using absorption and emission spectral studies. The absorption spectra of Zn-H<sub>8</sub>OCPP indicate the presence of a sharp Soret band at 420 nm and four weak Q-bands located at 515, 552, 593 and 644 nm (Fig. S5a). The absorption spectra of LnMPF-1s are characterized by broad Soret band due to exocyclic coordination of the metalloporphyrin moieties with the lanthanoid ions (Fig S5b, S5c).<sup>10a</sup> The emission

spectra of Zn-H<sub>8</sub>OCP, after excitation at 420 nm, consists of two emission bands at 647 [Q(0,0)] and 713 nm [Q(0,1)] (Fig. 5). It is interesting to note that the emission intensity of the Q(0,0) band is slightly lower as compared to that of the Q(0,1) band. The emission spectra of LnMPF-1 (Ln= Sm, Eu, Gd, and Tb) are shown in Fig. 5 as well. They show only the emission peaks related to the porphyrin building blocks due to their strong absorption in the UV region; whereas no peaks could be related to the lanthanide ions.<sup>10</sup>

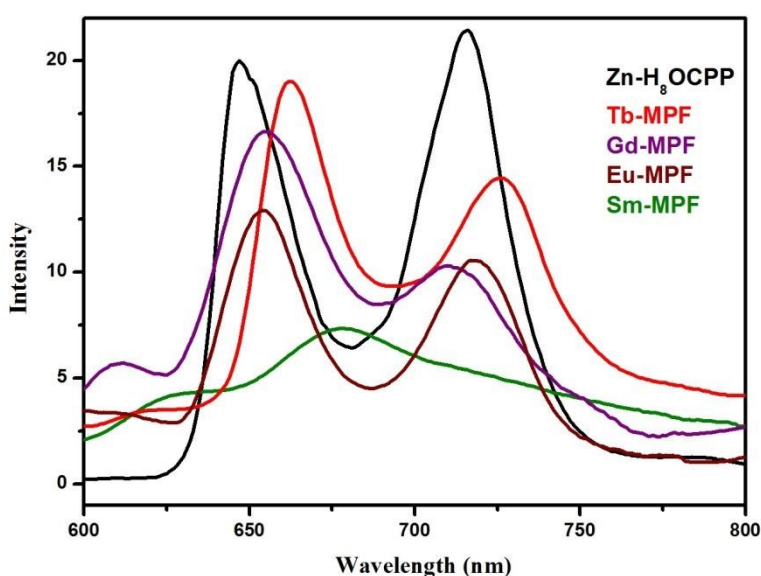


**Fig. 5** Fluorescence emission spectra of solid Zn-H<sub>8</sub>OCP and LnMPF-1 (Ln= Sm, Eu, Gd, and Tb) excited at 420 nm.

It appears that the optical properties (peak pattern) of the porphyrin component remained intact even after its incorporation into the MOF structures. However, noticeable red shifts and variation in the intensities of the bands were observed in the emission spectra of the MOFs, depending on the identity of the lanthanoid center. The emission spectra of TbMPF-1 depict major emission bands at 662 and 726 nm, which are characteristic of Zn-H<sub>8</sub>OCP, however with some interesting differences. Firstly, a red shift in Q(0,0) and Q(0,1) band is noted, and more importantly, the relative intensities of the Q(0,0) and Q(0,1) bands from the framework material are different than those of the free zinc-porphyrin ligand. The

excitation spectra of TbMPF-1 recorded at 661 nm (the maximum of emission spectrum) indicates that the effective energy of absorption is located in the range 375 to 418 nm. The emission spectra of GdMPF-1 also shows major emission bands related to porphyrin at 656 and 712 nm, with a red shift in Q(0,0) band and no shift in Q(0,1) band. In a similar way EuMPF-1 also display the emission bands at 653 and 718 nm, a slight red shift in both Q(0,0) and Q(0,1) bands. But in the more unique case of SmMPF-1, no major bands were observed but a broad emission peak in the range of 638-735 nm with emission maximum at 668 nm is observed.

A key difference was noted in terms of the intensity ratio of the two main bands Q(0,0)/Q(0,1), which is 1.61 in GdMPF-1, 1.31 in TbMPF-1, and 1.23 in EuMPF-1, when compared to 0.93 in the uncoordinated Zn-H<sub>8</sub>OCPP (an average of several measurements). This observation submits the role of lanthanoids in the emission spectra of these frameworks. In the few previously reported LnMPF-materials,<sup>10</sup> only characteristic emissions of the porphyrin (but not of the lanthanoid) moiety have been observed, in contrast with other non-porphyrin Ln-containing frameworks. In the latter energy transfer was commonly observed from the organic linkers to the lanthanoid metal centers, displaying characteristic lanthanide emissions.<sup>7</sup> However, in LnMPF-1s it appears that the Zn-H<sub>8</sub>OCPP linker does not transfer the energy absorbed to the metal centers. In a more intriguing fashion the coordinated lanthanoid center affects the intensity ratio between the two main bands in the emission spectra. It involves e.g. different quenching of the Q(0,1) band in the various compounds. More detailed studies are required to better quantify these spectral characteristics of the various framework materials. Individual absorption, emission and excitation spectra are shown in the supporting information.

### Concluding comments

In summary, we reported in this paper an improved synthetic procedure for the construction of unique 3D MOFs based on the octa-topic Zn-H<sub>8</sub>OCPP organic linkers and lanthanoid ions as nodes, by using NaOH as a modulator. The addition of excess amount of NaOH to the reaction mixture dwindle the reaction rate between porphyrin building block and lanthanoids, and improves the odds for obtaining sizeable crystals. Through this methodology we reported the first LnMPF-1 displaying permanent porosity and a unique architecture. The coordination linkage of the octa-topic

porphyrin ligand and the various lanthanoid ions result in the formation of (4,8) connected framework embedding 1D tubular zigzag channels of about 1.5 nm in diameter. The gas adsorption studies demonstrated the permanent porosity upon removal of solvent molecules. The emission spectra of the framework displays characteristic emission of porphyrin building blocks, but the intensity ratios and band shifts are dependent on the lanthanide metal center. The versatility of LnMPF-1s lies in terms of combination of lanthanides and porphyrins which are considered to be more prominent systems for light harvesting. In this context the synthetic methodology adopted in the article lay down a pathway for obtaining highly crystalline LnMPFs from the fast reacting porphyrin building blocks. Our ongoing work focuses on utilizing the materials presented here as potential candidates for light harvesting systems and also on efforts to obtain a wide variety of related LnMPFs with improved gas sorption capacity and specific photophysical features.

### Acknowledgements

This research was supported by the Israel Science Foundation (grant No. 108/12).

### Notes and references

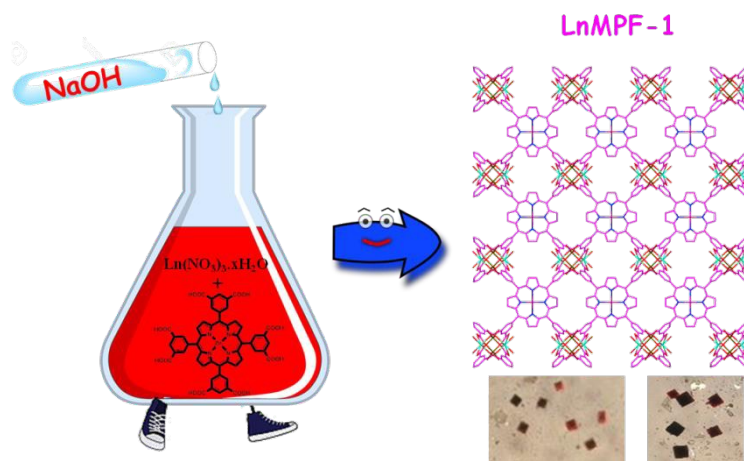
¶ Electronic supplementary information (ESI) available: Experimental details, luminescence spectra, PXRD, TG, and crystal data of the crystal structure determinations of compounds **1-4** (CCDC 1422227-1422230 for **1-4**, respectively). For ESI and crystallographic data in CIF and or other electronic format see DOI: 10.1039/xxxxxxxxxx.

1. (a) J. S. Lindsey, *The Porphyrin Handbook*, ed. K. M. Kadish, K. M. Smith and R. Guilard, Academic Press, San Diego, 2000, vol. 1, pp. 45–118; (b) *The Porphyrin Handbook*, ed. K. M. Kadish, K. M. Smith and R. Guilard, Academic Press, San Diego, 2000–2003.
2. (a) H. Mori, T. Tanaka, S. Lee, J.M. Lim, D. Kim and A. Osuka, *J. Am. Chem. Soc.*, 2015, **137**, 2097; (b) K. Gao, L.Li, T. Lai, L. Xiao, Y. Huang, F. Huang, J. Peng, Y. Cao, F. Liu, T. P. Russell, R. A. J. Janssen and X. Peng, *J. Am. Chem. Soc.*, 2015, **137**, 7282; (c) F. X. Redl, M. Lutz and J. Daub, *Chem. Eur. J.*, 2001, **7**, 5350.

3. (a) H.-J. Son, S. Jin, S. Patwardhan, S. J. Wezenberg, N. C. Jeong, M. So, C. E. Wilmer, A. A. Sarjeant, G. C. Schatz, R. Q. Snurr, O. K. Farha, G.P. Wiederrecht and J. T. Hupp, *J. Am. Chem. Soc.* 2013, **135**, 862; (b) M.-S. Choi, T. Yamazaki, and I. Yamazaki, T. Aida, *Angew. Chem. Int. Ed.*, 2004, **43**, 150; (c) Y. Chen, T. Hoang and S. Ma *Inorg. Chem.*, 2012, **51**, 12600; d) M. Jahan, Q. Bao and K. P. Loh, *J. Am. Chem. Soc.*, 2012, **134**, 6707.
4. (a) D. Liu, T.-F. Liu, Y.-P. Chen, L. Zou, D. Feng, K. Wang, Q. Zhang, S. Yuan, C. Zhong and H.-C. Zhou, *J. Am. Chem. Soc.* 2015, **137**, 7740; (b) X.-S. Wang, L. Meng, Q. Cheng, C. Kim, L. Wojtas, M. Chrzanowski, Y.-S. Chen, X. P. Zhang, and S. Ma *J. Am. Chem. Soc.* 2011, **133**, 16322.
5. (a) M.-H. Xie, X.-L. Yang, Y. He, J. Zhang, B. Chen and C.-D. Wu *Chem. Eur. J.*, 2013, **19**, 14316; (b) M. Otte, P. F. Kuijpers, D.-C. O. Troeppner, I. I. Burmazović, J. N. H. Reek and B. de Bruin, *Chem. Eur. J.*, 2013, **19**, 10170.
6. S. Jin, H.-J. Son, O. K. Farha G. P. Wiederrecht and J. T. Hupp *J. Am. Chem. Soc.* 2013, **135**, 955.
7. a) P. P. Bag, X.-S. Wang and R. Cao, *Dalton trans.* 2015, **44**, 11954; (b) S. Dang, X. Min, W. Yang, F.-Y. Yi, H. You and Z.-M. Sun, *Chem. Eur. J.*, 2013, **19**, 17172; (c) P. Wang, J.-P. Ma and Y.-B. Dong, *Chem. Eur. J.*, 2009, **15**, 10432–10445.
8. (a) S. Muniappan, S. Lipstman, S. George and I. Goldberg, *Inorg. Chem.* **2007**, **46**, 5544; (b) S. Lipstman, S. Muniappan, S. George and I. Goldberg, *Dalton Trans.* 2007, **30**, 3273; (c) S. Lipstman and I. Goldberg, *Israel J. Mol. Struct.* **2008**, **890**, 101.
9. G. Nandi and I. Goldberg, *Chem. Commun.*, 2014, **50**, 13612.
10. (a) J. Demel, P. Kubát, F. Millange, J. Marrot, I. Císařová and K. Lang, *Inorg. Chem.*, 2013, **52**, 2779; (b) W.-T. Chen, Z.-G. Luo, Y.-F. Wang, X. Zhang and H.-R. Fu, *Inorg. Chim. Acta*, 2014, **414**, 1; (c) W.-T. Chen, R.-H. Hu, Y.-F. Wang, X. Zhang and J. Liu, *J. Solid State Chem.*, 2014, **213**, 218.
11. (a) T. Zhang, X. Zhu, W.-K. Wong, H.-L. Tam and W.-Y. Wong, *Chem. Eur. J.*, 2012, **19**, 739; (b) D. Feng, Z.-Y. Gu, J.-R. Li, H.-L. Jiang, Z. Wei and H.-C. Zhou, *Angew. Chem. Int. Ed.*, 2012, **51**, 10307.
12. (a) X.S. Wang, M. Chrzanowski, C. Kim, W.-Y. Gao, L. Wojtas, Y.-S. Chen, X. P. Zhang and S. Ma *Chem. Commun.*, 2012, **48**, 7173; (b) X.-L. Yang, M.-H. Xie, C. Zou, Y. He, B. Chen, M. O’Keeffe and C.-De Wu, *J. Am. Chem. Soc.*,

- 2012, **134**, 10638; (c) X.-L. Yang and C.-D. Wu, *Inorg. Chem.*, 2014, **53**, 4797; (d) X.-L. Yang, C. Zou, Y. He, M. Zhao, B. Chen, S. Xiang, M. O’Keeffe and C.-D. Wu, *Chem. Eur. J.*, **2014**, *20*, 1447–1452; (e) X.S. Wang, M. Chrzanowski, W.-Y. Gao, L. Wojtas, Y.-S. Chen, M. J. Zaworotko and S. Ma, *Chem. Sci.*, 2012, **3**, 2823; (f) X.S. Wang, M. Chrzanowski, L. Wojtas, Y.-S. Chen and S. Ma, *Chem. Eur. J.*, 2013, **19**, 3297.
13. (a) A. Schaate, P. Roy, A. Godt, J. Lippke, F. Waltz, M. Wiebcke and P. Behrens, *Chem. Eur. J.*, 2011, **17**, 6643. (b) S. B. Kalidindi, S. Nayak, M. E. Briggs, S. Jansat, A. P. Katsoulidis, G. J. Miller, J. E. Warren, D. Antypov, F. Cor, B. Slater, M. R. Prestly, C. M.-Gastaldo and M. J. Rosseinsky *Angew. Chem. Int. Ed.* 2015, **54**, 221.
14. (a) H.-L. Jiang, D. Feng, K. Wang, Z.-Y. Gu, Z. Wei, Y.-P. Chen and H.-C. Zhou, *J. Am. Chem. Soc.*, 2013, **135**, 13934; (b) T. F.u Liu, D. Feng, Y.-P. Chen, L. Zou, M. Bosch, S. Yuan, Z. Wei, S. Fordham, K. Wang and H.-C. Zhou, *J. Am. Chem. Soc.*, 2015, **137**, 413.
15. A. L. Spek, *Acta Cryst.*, 2015, **C71**, 9.
16. (a) V. A. Blatov, *Struct. Chem.*, 2012, **23**, 955; (b) M. O’Keeffe, M. A. Peskov, S. J. Ramsden and O. M. Yaghi, *Acc. Chem. Res.*, 2008, **41**, 1782; (c) O. Delgado Friedrichs, M. O’Keeffe and O. M. Yaghi, *Acta Cryst.*, 2003, **A59**, 22.
17. Z. Guo, D. Yan, H. Wang, D. Tesfagaber, X. Li, Y. Chen, W. Huang and B. Chen, *Inorg. Chem.*, 2015, **54**, 200.

For the Table of Contents



**Let the MOF's crystals grow!** Novel synthetic methodology has been applied to obtain sizeable single crystallites of lanthanide metalloporphyrins from the octa-topic octa-carboxylate porphyrin linker. The obtained materials show permanent porosity and appealing photophysical behavior. This methodology lays down a pathway to obtain lanthanide metalloporphyrins with a wider variety of the porphyrin scaffolds.